JOURNAL OF OPTOELECTRONICS AND ADVANCED MATERIALS Vol. 15, No. 9 - 10, September – October 2013, p. 971 - 975

Enhanced red emission in Eu^{3+} doped fluoro-borosilicate glass by introducing ZnF_2

XUEAN ZHANG[a], SIGUO XIAO[a, b*], XIAOLIANG YANG[a,b], XIANGLIANG JIN[a,b]
[a]*Faculty of Materials, Optoelectronics and Physics, Institute for Nanophysics and Rare-earth Luminescence, Xiangtan University, Xiangtan 411105, P. R. China*
[b]*Faculty of Materials, Optoelectronics and Physics, Xiangtan University, Xiangtan 411105, P. R. China*

The ZnF_2 content dependent glass structure has been discussed based on fourier-transform infrared spectroscopy. The influence of ZnF_2/ZnO ratio on the optical properties of Eu^{3+}-doped fluoro-borosilicate glass has been investigated. It is found that the red emission increases with the enhancement of ZnF_2/ZnO ratio. The Judd–Ofelt (J-O) parameters (Ω_2, Ω_4) have been evaluated from the recorded emission spectra. The Ω_2 and Ω_4 parameters increase with the ZnF_2/ZnO ratio, due to the increased symmetry of Eu^{3+} sites.

(Received December 21, 2012; accepted September 18, 2013)

Keywords: Fluoro-borosilicate glass; Eu^{3+}; luminescence

1. Introduction

Rare-earth ions doped oxyfluoride glasses are important materials for bulk lasers, optical fibers, waveguide lasers, optical amplifiers, sensors and so on[1-4], because of their excellent optical and properties including high refractive index, low dispersion and good transparency in the UV and IR regions and good chemical and thermal stability [1-5].

B_2O_3 is a typical glass former for both oxide and oxyfluoride glasses due to its higher bond strength, lower cation size and smaller heat of fusion. However, the structure of borate glasses is completely different from other glasses such as phosphate and silicate glasses. The structure of borate glasses mainly consists of $[BO_{3/2}]^0$, $[BO_{4/2}]^-$. Moreover, the concentrations of $[BO_{3/2}]^0$, $[BO_{4/2}]^-$ depend on the amount of and the characteristics of the modifiers presented in the glass system [6].

Addition of fluoride into the borate glass matrix is expected to lower the viscosity and liquidus temperature to a substantial extent, which is helpful for glass formation. Further, earlier studies have shown that the presence of fluoride compounds like zinc fluorides in the glass matrices, increases the glass-forming region due to the complicated constituent composition of the glass matrix [7-11].

On the other hand, optical properties of rare-earth (RE) ions doped into various oxyfluoride glasses have been studied widely in the last several decades [12-19]. Eu^{3+} is an important and efficient luminescence centre in the oxyfluoride host, due to its simple electronic energy level scheme and large energy gap between the ground state and its emissive state. Eu^{3+} is also one of the most important ions applied as spectroscopic probe because it can exhibit pure magnetic and electric dipole transitions, which can provide information on the glass structure and nature of local environment of luminescence centre in glasses [20].

In this work, ZnO/ZnF_2-B_2O_3-SiO_2-K_2O-CaO-Al_2O_3:Eu_2O_3 fluoro-borosilicate glass has been prepared. X-ray diffraction (XRD), Fourier-transform infrared (FT-IR) spectroscopy and luminescence spectra have been measured. The ZnF_2/ZnO ratio dependent luminescence properties of Eu^{3+} have been discussed.

2. Experiment

Fluoro-borosilicate glasses with the molar composition of (40-x)ZnO-x ZnF_2-$40B_2O_3$-$10SiO_2$-$5K_2O$-5CaO-$10Al_2O_3$: $2Eu_2O_3$ (where x =0, 10, 20, 30, and 40 mol%) were prepared by conventional melt quenching technique. Analar grade chemicals K_2CO_3, ZnO, ZnF_2, SiO_2, $CaCO_3$, Al_2O_3, B_2O_3 and Eu_2O_3 were used as starting materials. The chemicals of the required compositions of approximately 10 g were weighed in an electronic balance and grounded in an agate mortar to get a fine powder. The batches of the raw materials were melted at 1250–1300 °C for 30 min in a covered corundum crucible in normal atmosphere. The melt was in air poured onto a brass mould and then pressed by another brass plate at room temperature in air and transparent glass was obtained. The glasses with different ZnO/ZnF_2 ratio are labeled as G1, G2, G3, G4 and G5 for x=0, 10, 20, 30 and 40 mol%, respectively.

The prepared transparent glass samples were ground into powders and sieved using 200 mesh sieves to be used for different measurement including X-ray diffraction (XRD), Fourier-transform infrared (FT-IR) and photoluminescence (PL).

The structure of the glass was determined by XRD using Rigaku D/MAX 2500 vertical goniometer with Cu Kα radiation (λ = 1.54 Å) operated at 40 kV/200 mA and scanned in the range of 10–90° with a step of 0.02°. Excitation and emission luminescence spectra were analyzed with a Hitachi F-4500 fluorescence spectrophotometer using a 150 W xenon lamp as the excitation source at room temperature. IR transmission spectra of the glasses were measured in the range 400 - 1600 cm^{-1} using a fourier transform computerized infrared spectrometer (type Thermo Nicolet 380 spectrometer). For the measurement, 1 mg of each sample was mixed with 100 mg KBr in an agate mortar, and then pressed into a tablet. A spectral resolution of 4 cm^{-1} was chosen, and the spectrum of each sample represented an average of 100 scans with substracting the blank KBr spectrum. All the above spectral measurements were performed at room temperature.

3. Results and discussion

The XRD patterns given in Fig. 1 show the structural of the G4 sample. Broad diffraction bands at 2θ = 32° and 42° can be seen. The glass powders exhibit typical broad diffraction maxima of an amorphous structure and no obvious crystalline peaks can be found within the XRD resolution limits. The diffraction patterns of other samples are similar, suggesting that all the samples are amorphous.

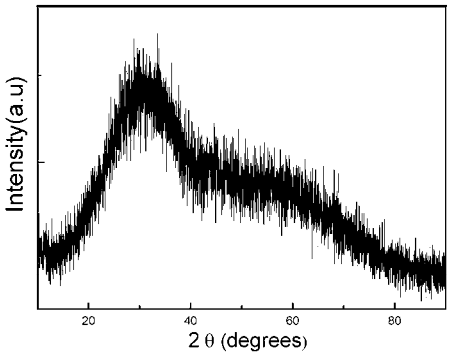

Fig. 1 X-Ray diffraction pattern of fluoro-borosilicate glass.

Fig. 2 presents the FT-IR spectra of Eu^{3+}-doped fluoro-borosilicate glasses in the range from 400-1600 cm^{-1}. The vibrational spectra associated with the fluoro-borosilicate glasses are divided into several spectral regions. The band located in the region of 1200-1600 cm^{-1} is due to the asymmetric stretching relaxation of the B-O band of trigonal BO_3 units. The region from 800 to 1200 cm^{-1} corresponds to B-O stretching vibrations of BO_4 tetrahedral units. The region located at about 697 cm^{-1} result from the bending of B-O-B linkages in the borate network [2, 21-23].

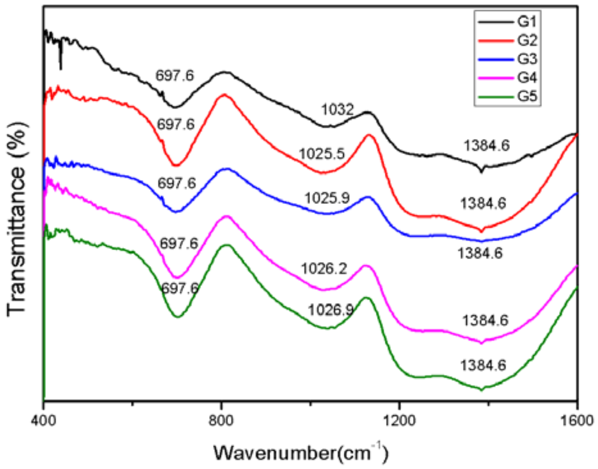

Fig. 2 FTIR spectra of Eu^{3+} doped fluoro-borosilicate glasses containing different ZnF_2/ZnO ratio.

For no ZnF_2 sample, the peak of the FT-IR band ascribing to the BO_4 vibration locates at 1032cm^{-1}. With the introduction of ZnF_2, red-shifts can be observed. Presumably, the tiny change might result from the BOF_3 groups or BO_2F_2 groups formed in the glass with addition of ZnF_2. M. El-Hofy et al [24] have reported that the B-O bond length and the B-F bond length are 0.164-0.175 nm and 0.149-0.159 nm respectively. This means that the B–O bond is longer than the B-F bond. The change for the symmetry of the BO_4 groups occurred when the F-ions replace O-ion in BO_4 unit, leading to the shift of the vibrational band. The probable linkages between BO_4 units with introduction fluoride are shown in Fig. 3. It is to be noted in the figure that the borate groups are connected by oxygen and the K^+ ion will be located near the fluorine and at non-bridging oxygens to serve as charge compensator. When ZnF_2 is introduced, part of O-ions in BO_4 units is replaced by F-ions.

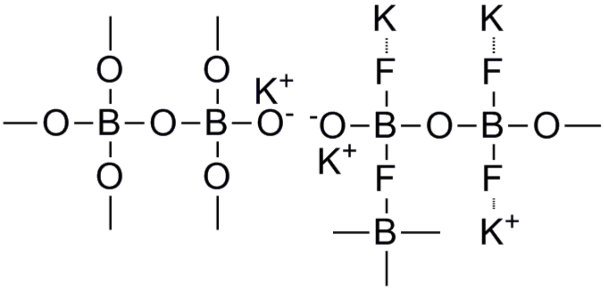

Fig. 3 A Schematic illustration of fluoro-borosilicate glasse.

In Fig. 2, however, no shift has been observed and relative band intensity has also not varied in the region of 1200-1600 cm^{-1}. This indicates that the BO_3 units hardly change. The result means that F-ions tend to substitute O-ion in BO_4 units rather than that in BO_3 units. The reason lies in that the B-O bond length in BO_3 units is shorter than that in BO_4 units [24]. Therefore, the B-O bond strength in BO_3 units is stronger than the B-O bond strength in BO_4 units. As a result, the F-ions might be difficult to substitute the O-ion site in BO_3 units, but easy to substitute the O-ion site in BO_4 units. Consequently, Red-shift of the FT-IR band corresponding to the BO_4 units can be observed with increasing of the introduced ZnF_2 content, while no evident change of the FT-IR band corresponding to the BO_3 units can be observed.

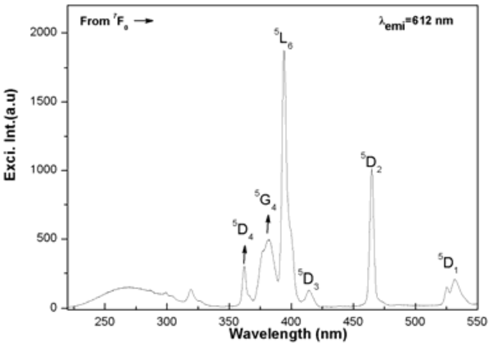

Fig. 4 Excitation spectra (λ_{eni}= 612 nm) of Eu^{3+}-doped fluoro-borosilicate glass at room temperature.

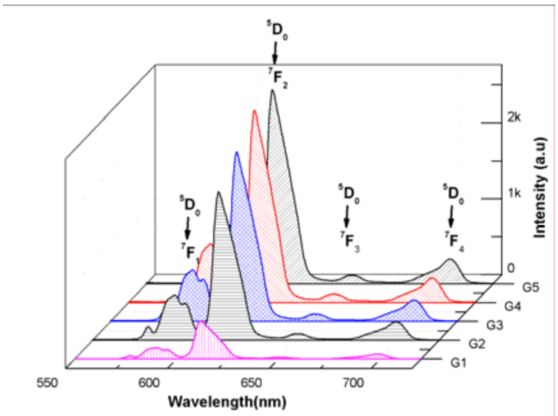

Fig. 5 Emission spectra (λ_{exc}=395 nm) of Eu^{3+}-doped fluoro-borosilicate glasses at room temperature.

Fig. 4 shows the room-temperature excitation spectra of the G2 sample in which the amount of ZnF_2 is 30% in mole. The excitation spectra is measured in the wavelength range 200-550 nm by monitoring with an intense red emission located at 612 nm of $^5D_0$→$^7F_2$ transitions. The spectral range from 200 to 550 nm consists of sharp lines, which resulted from transitions between the 4f energy levels of Eu^{3+}. The excitation bands can be assigned to $^7F_0$→$^5D_1$ (534 nm), $^7F_0$→$^5D_2$ (465 nm), $^7F_0$→$^5D_3$ (414 nm), $^7F_0$→$^5L_6$ (395 nm), $^7F_0$→$^5G_3$ (383 nm) and $^7F_0$→$^5D_4$ (362 nm) [25, 26].

Fig. 5 shows emission spectra (excited at 395 nm) of Eu^{3+} doped fluoro-borosilicate glasses with various amount of ZnF_2 in raw materials. The spectra consist of some well-known $^5D_0$→^7F_J (J=0, 1, 2, 3 and 4) transitions namely $^5D_0$→$^7F_0$ (576 nm), $^5D_0$→$^7F_1$ (590 nm), $^5D_0$→$^7F_2$ (612 nm), $^5D_0$→$^7F_3$ (650 nm) and $^5D_0$→$^7F_4$ (699 nm), respectively. Fig. 6 shows the possible emission transitions of Eu^{3+} ion in the fluoro-borosilicate glasses. The transitions $^5D_0$→^7F_J with J = 5 and 6 are not observed as transition probabilities are very weak. It also can be seen from Fig.5 that with increasing ZnF_2 concentrations, the emission peaks intensity at 590 nm and 612nm gradually increased, meaning the f-f transition of Eu^{3+} increases with the ZnF_2/ZnO ratio. However, for the higher ZnF_2 content, the glass becomes opaque.

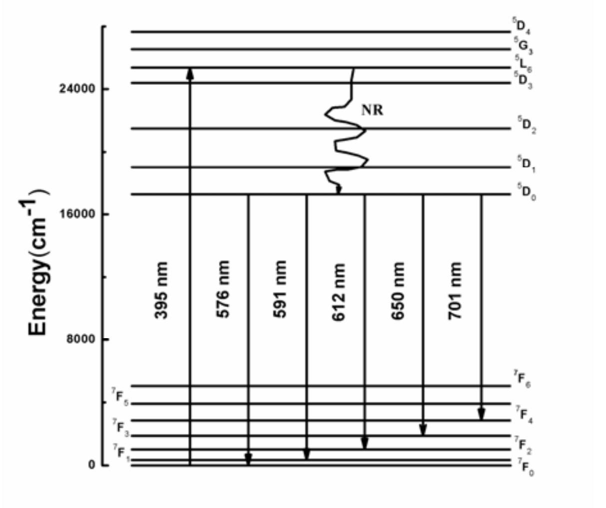

Fig. 6 Energy level diagram showing emission transitions of Eu^{3+} ions in the fluoro-borosilicate glass.

It is known that the spontaneous emission probability (A) of the transition *ψJ →ψ'J'* is written as the following equation [27],

$$A(\psi J,\psi' J') = \frac{64\pi^4}{3h}\frac{\nu^3}{2J'+1}\left[\frac{n(n^2+2)^2}{9}D_{ED} + n^3 D_{MD}\right] \tag{1}$$

where υ_{avg} is the average transition energy in cm^{-1}, *h* is Planck constant (6.631×0^{-27} erg s), 2*J* +1 is the degeneracy of the initial state (1 for $^5D_0$). D_{ED} and D_{MD} are the electric and magnetic dipole strength (in esu^2 cm^2), respectively. The factors containing medium's refractive index *n* result from local field corrections that convert the external electromagnetic field into an effective field at the location of the active center in the dielectric medium.

For Eu^{3+} ion, the transition $^5D_0$ to $^7F_1$ is a magnetic dipole one, and has no electric dipole contribution. Magnetic dipole transitions in lanthanide ions are practically independent of the ion's surroundings. The strength intensity the transition $^5D_0$ to $^7F_1$ of Eu^{3+} has been well calculated in theory (D_{MD} $=9.6\times10^{-42}$ esu^2 cm^2 = 9×10^{-6} D^2) .

The $^5D_0$ to $^7F_{,2,}$ and $^7F_{,3}$ transitions are purely induced electric dipole ones, and the strength of all induced dipole transitions can be calculated on basis of only three phenomenological parameters Ω_λ according to J-O theory[28, 29]. The strength of induced dipole transitions can be expressed as

$$D_{ED} = e^2 \sum_{\lambda=2,4,6} \Omega_\lambda \left|\langle\psi J\|U^{(\lambda)}\|\psi' J'\rangle\right|^2 \tag{2}$$

where e stands for elementary charge e and $\left|\langle\psi J\|U^{(\lambda)}\|\psi' J'\rangle\right|^2$ are the squared reduced matrix elements whose values are independent of the environment of the ion. For the case of Eu^{3+} these values are given in Table 1 according to Refs.[30, 31].

Table 1 Squared reduced matrix elements used for the calculation of dipole strengths of the allowed induced ED transitions in the emission spectra of Eu^{3+}.

$^5D_0\rightarrow$	$\langle\psi J\|U^2\|\psi$	$\langle\psi J\|U^4\|\psi' J'$	$\langle\psi J\|U^6\|\psi' J'$
$^7F_2$	0.0032	0	0
$^7F_4$	0	0.0023	0
$^7F6$	0	0	0.0002

Thus the phenomenological parameters Ω_2 and Ω_4 , can be calculated from the ratio of the intensity of the ^5D $\rightarrow ^7F_\lambda$ (λ= 2, 4 and 6) transitions $\int I_\lambda(\nu)d\nu$ to the intensity of the $^5D\rightarrow{}^7F_1$ transition $\int I_1(\nu)d\nu$, i.e.,

$$\Omega_\lambda = \frac{D_{MD}\nu_1^3}{e^2\nu_\lambda^3}\frac{9n^3}{n(n^2+2)^2}\frac{1}{|\langle\psi J\|U^\lambda\|\psi' J'\rangle|^2}\times\frac{\int I_\lambda(\nu)d\nu}{\int I_1(\nu)d\nu} \tag{3}$$

The J-O intensity parameters Ω_2 and Ω_4 are calculated from the emission spectra of Eu^{3+} for all the samples. The ZnF_2 content dependent J-O parameters are given in Fig 7.

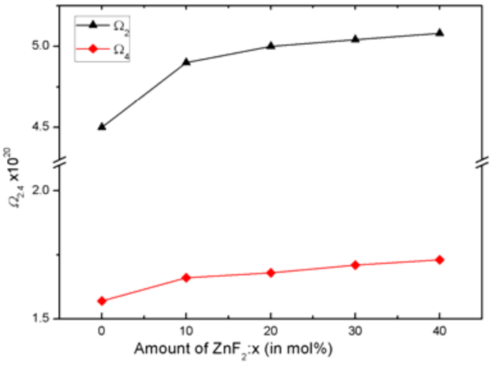

Fig. 7 Ω_2 and Ω_4 as a function of ZnF_2 content.

In Fig. 7, one may find that the parameters Ω_2 and Ω_4 both increase with increasing ZnF_2 content. Moreover, the value of Ω_2 has a more significant growth than that of Ω_4. It is known that the Ω_2 parameter depends on both asymmetry and covalency at the rare earth ion sites [32, 33]. Ω_4 parameter is affected by the factors causing changes in both the Ω_2 and Ω_6 parameters [34]. This means that the variation of Ω_2 can more reflect the change of the local environment of Eu^{3+}. With the increase of the ZnF_2 content, more and more oxygen ligands for Eu^{3+} sites are replaced by fluorine ions. As a result, the asymmetry of Eu^{3+} sites increases, leading to the increase of value of Ω_2 and thus the increase of Ω_4.

4. Conclusion

The influence of ZnF_2 content on the glass structure and optical properties of Eu^{3+}-doped fluoro-borosilicate glasses has been investigated. It is believed that the introduced fluoride can result in the formation of the BOF_3 groups or BO_2F_2 groups in glass. With the ZnF_2 content increasing, the asymmetry of Eu^{3+} sites increases. Consequently, the red emission increases with the ZnF_2/ZnO ratio. The work refers a possible way to improve and adjust the luminescence properties of rare earth doped glass.

Acknowledgement

This work is supported by National Natural Science Foundation of China (No.51372214), Hunan Provincial Natural Science Foundation of China (No.11JJ2036 & 12JJ3063).

References

[1] D. L. Sidebottom, P. F. Green, R. K. Brow, J. Non-Cryst. Solids. **222,** 354 (1997).
[2] S. Rada, V. Dan, M. Rada, E. Culea, J. Non-Cryst. Solids. **356**, 474 (2010).
[3] Z. G. Ivanova, M. Jayasimhadri, M. Kincl, J. Optoelectron. Adv. Mater. **11**, 1269 (2009).
[4] B. Hari Babu, V. V. Ravi Kanth Kumar, J. Appl. Phys. **112**, 093516 (2012).
[5] M. J. Dejneka, Mater. Res. Bull. **23**, 57 (1998)
[6] I. Ardeleana, M. Toderas, J. Optoelectron. Adv. Mater. **8**(3)**,** 1118 (2006).
[7] M. Poulain, M. Poulain, Mater. Res. Bull. **10**, 243 (1975).
[8] Yu-Hu Wang, J. Takada, K. Oda, K. Takahasha, Mater. Sci. Forum. **32**, 97 (1972).
[9] D. K. Durga, P. Yadagiri Reddy, N. Veeraiah, J. Lumin. **99**, 53 (2002).
[10] N. A. Toropov, I. A. Bondar, F. Y. Galadhov, K. S. Nikogosyan, N. V. Vinogradova, Bulletin of the Academy of Sciences of the USSR, Division of chemical science, **13,** 1076 (1964).
[11] D. K. Durga and N. Veeraiah, Phys. Rev. B. **324**, 127 (2002).
[12] Z. Duan, J. Zhang, D. He, H. Sun, L. Hu, Mater. Chem. Phys. **100**, 400 (2006).
[13] J. Qiu, Z. Song, J. Rare Earths. **26,** 919 (2008).
[14] S. González-Pérez, I. R. Martín, D. Jaque, P. Haro-González, N. Capuj, J. Appl. Phys. **108**, 103103 (2010).
[15] Maurício A. P. Silva, Geraldine Dantelle, Michel Mortier, André Monteil, Sidney J. L. Ribeiro, Younès Messaddeq, Valérie Briois, Marcel Poulain, J. Chem. Phys. **128**, 244516 (2008).
[16] Zhongchao Duan, Junjie Zhang, Lili Hu, J. Appl. Phys. **101**. 043110 (2007).
[17] Y. Kuisheng, X. Huili, W. Rinang, K. Jiaqiang, W. Weizhong, Z. Bin, Z. Xiyan, J. Rare Earths. **24,** 175 (2006).
[18] P. Pascuta, M. Bosca, S. Rada, L. Pop, E. Culea, J. Optoelectron. Adv. Mater. **10**, 2210 (2008).
[19] Yisheng Dai, Toshiyasu Kawaguchi, Koichi Suzuki, Susumu Suzuki, Kiyoshi Yamamoto, Akio Masui, Appl. Phys. Lett. **58**, 422 (1991).
[20] K. Driesen, V. K. Tikhomirov, C. Go□rller-Walrand, J. Appl. Phys. **102**, 024312 (2007).
[21] S. Ram, K. Ram, J. Mater. Sci. **23**, 4541 (1988)
[22] M. Ganguli, K. J. Rao, J. Solid State Chem. **145**, 65(1999).
[23] S. Rada, E. Culea, M. Neumann, J. Mol. Model. **16**, 1333 (2010).
[24] I. Z. Hager and M. El Hofy, Phys. Status. Solidi. A. **198**, 7 (2003).
[25] P. Babu, C. K. Jayasankar, Phys. Rev. B. **279**, 262 (2000).
[26] S. Hufner, B. R. Judd, Phys. Today. **32**, 76 (1979).
[27] M. H. V. Werts, R. T. F. Jukes, J. W. Verhoeven, Phys. Chem. Chem. Phys. **4**, 1542 (2002).
[28] B. R. Judd, Phys. Rev. **127**, 750 (1962).
[29] G. S. Ofelt, J. Chem. Phys. **37**, 511 (1962).
[30] S. Tirtha, K. Basudeb, J. Phys.: Condens. Matter. **22,** 035603 (2010).
[31] W. T. Carnall, H. Crosswhite, H. M. Crosswhite, Argonne Natl. Lab. Rept. (1977).
[32] T. Som, B. Karmakar, J. Phys. Condens. Matter. **22**, 035603 (2010).
[33] Z. Jiang, Y. Jianhu, D. Shixun, J. Opt. Soc. Am. B, **21**, 739 (2004).
[34] V. Nazabal, S. Todoroki, A. Nukui, T. Matsumoto, S. Suehara, J. Non-Cryst. Solids, **325**, 85 (2003).

---

[*] Corresponding author: xiaosiguo@xtu.edu.cn